

# One-proton and one-neutron knockout reactions from $N = Z = 28$ $^{56}\text{Ni}$ to the $A = 55$ mirror pair $^{55}\text{Co}$ and $^{55}\text{Ni}$

M. Spieker,<sup>1,\*</sup> A. Gade,<sup>1,2</sup> D. Weisshaar,<sup>1</sup> B. A. Brown,<sup>1,2</sup> J. A. Tostevin,<sup>3</sup> B. Longfellow,<sup>1,2</sup> P. Adrich,<sup>1,†</sup> D. Bazin,<sup>1,2</sup> M. A. Bentley,<sup>4</sup> J. R. Brown,<sup>4</sup> C. M. Campbell,<sup>1,2,‡</sup> C. Aa. Diget,<sup>4</sup> B. Elman,<sup>1,2</sup> T. Glasmacher,<sup>1,2</sup> M. Hill,<sup>1,2</sup> B. Pritychenko,<sup>5</sup> A. Ratkiewicz,<sup>1,2,§</sup> and D. Rhodes<sup>1,2</sup>

<sup>1</sup>National Superconducting Cyclotron Laboratory, Michigan State University, East Lansing, Michigan 48824, USA

<sup>2</sup>Department of Physics and Astronomy, Michigan State University, East Lansing, Michigan 48824, USA

<sup>3</sup>Department of Physics, Faculty of Engineering and Physical Sciences, University of Surrey, Guildford, Surrey GU2 7XH, United Kingdom

<sup>4</sup>Department of Physics, University of York, Heslington, York YO10 5DD, United Kingdom

<sup>5</sup>National Nuclear Data Center, Brookhaven National Laboratory, Upton, New York 11973, USA



(Received 25 March 2019; published 22 May 2019)

We present a high-resolution in-beam  $\gamma$ -ray spectroscopy study of excited states in the mirror nuclei  $^{55}\text{Co}$  and  $^{55}\text{Ni}$  following one-nucleon knockout from a projectile beam of  $^{56}\text{Ni}$ . The newly determined partial cross sections and the  $\gamma$ -decay properties of excited states provide a test of state-of-the-art nuclear structure models and probe mirror symmetry in unique ways. The new experimental data are compared to large-scale shell-model calculations in the full  $pf$  space which include charge-dependent contributions. A mirror asymmetry for the partial cross sections leading to the two lowest  $3/2^-$  states in the  $A = 55$  mirror pair was identified as well as a significant difference in the  $E1$  decays from the  $1/2_1^+$  state to the same two  $3/2^-$  states. The mirror asymmetry in the partial cross sections cannot be reconciled with the present shell-model picture or small mixing introduced in a two-state model. The observed mirror asymmetry in the  $E1$  decay pattern, however, points at stronger mixing between the two lowest  $3/2^-$  states in  $^{55}\text{Co}$  than in its mirror  $^{55}\text{Ni}$ .

DOI: [10.1103/PhysRevC.99.051304](https://doi.org/10.1103/PhysRevC.99.051304)

The concept of isospin symmetry in atomic nuclei is rooted in the fundamental assumption of charge symmetry and charge independence of the attractive nucleon-nucleon interaction, see the review article [1]. In the absence of isospin-breaking effects, such as the Coulomb force, an exact degeneracy of isobaric analog states (IASs) with isospin quantum number  $T$  in nuclei of the same mass but with interchanged neutron and proton numbers (mirror pairs) would be expected. Thus, observed differences of IAS properties in mirror nuclei can elucidate the presence and nature of isospin-breaking contributions to the nuclear many-body problem. Excitation-energy shifts between mirror pairs, so-called mirror energy differences (MED), were systematically studied to identify such contributions in the  $pf$  shell [2,3], i.e., for nuclei between the doubly magic  $N = Z$  nuclei  $^{40}\text{Ca}$  and  $^{56}\text{Ni}$ . Unexpected asymmetries in the  $E1$  decay pattern of low-lying excited states were also observed between mirror pairs [4–7]. Their origin has been traced back to isospin-symmetry

violation though the exact underlying mechanism is still discussed [8,9].

We report on a study that uses mirrored one-neutron and one-proton knockout reactions from  $^{56}\text{Ni}$  to the mirror nuclei  $^{55}\text{Ni}$  and  $^{55}\text{Co}$ , respectively. Similar types of mirrored reactions have been employed before to extract MED in more distant mirror pairs such as ( $^{52}\text{Ni}$ ,  $^{52}\text{Cr}$ ) [10], ( $^{53}\text{Ni}$ ,  $^{53}\text{Mn}$ ) [11], and ( $^{70}\text{Se}$ ,  $^{70}\text{Kr}$ ) [12]; however, they started from projectiles that are mirrors themselves rather than from a self-conjugate nucleus. Brown *et al.* [13] used the  $\gamma$ -ray spectra of  $^{53}\text{Ni}$  and  $^{53}\text{Mn}$  from the three-neutron and three-proton removal on  $^{56}\text{Ni}$  projectiles to match analog states but such reactions cannot be described within a direct reaction formalism.

The doubly magic nucleus  $^{56}\text{Ni}$  and the  $T = 1/2$  ( $T_z = \pm 1/2$ ) ( $^{55}\text{Co}$ ,  $^{55}\text{Ni}$ ) mirror pair are of particular interest as they are coming within reach of *ab initio*-type calculations [14,15] that compute nuclei based on forces from chiral effective field theory.  $^{56}\text{Ni}$  has also been a target for early large-scale configuration-interaction shell-model calculations in the full  $pf$  model space [16], pioneering coupled-cluster calculations [17,18], and self-consistent Green's function theory [19,20]. Although nominally doubly magic,  $^{56}\text{Ni}$  behaves as a soft core in shell-model calculations performed in the full  $pf$  model space. Using the effective isospin-conserving GXPF1A interaction, the closed-shell  $(1f_{7/2})^{16}$  configuration comprises only about 68% of the ground-state wave function [21]. These calculations successfully account for the observed quadrupole collectivity [22] and the ground-state magnetic moments of

\* spieker@nsl.msu.edu

<sup>†</sup>Present address: National Centre for Nuclear Research, Otwock, Poland.

<sup>‡</sup>Present address: Nuclear Science Division, Lawrence Berkeley National Laboratory, Berkeley, California 94720, USA.

<sup>§</sup>Present address: Lawrence Livermore National Laboratory, Livermore, California, 94550, USA.

the odd- $A$  neighbors with one nucleon added or removed [23–26].

In terms of single-particle properties, a number of experiments [27–36] and theoretical studies [16,17,19–21,37,38] have been performed to identify the fragments of the single-particle levels relative to the  $N = Z = 28$  core and have also suggested the existence of  $2_1^+(^{56,58}\text{Ni}) \otimes 1f_{7/2}^{-1}$  core-coupled excitations with  $J^\pi = 3/2^-, \dots, 11/2^-$  in the vicinity of  $^{56}\text{Ni}$  [39–41]. Only recently, an inverse-kinematics one-neutron transfer experiment  $^1\text{H}(^{56}\text{Ni}, d)^{55}\text{Ni}$  populated for the first time single-hole-like states directly from the  $^{56}\text{Ni}$  ground state [36], however, without detecting subsequent  $\gamma$ -ray emission. An excited  $3/2^-$  and excited  $1/2^+$  state were observed.

Relevant to this work, strong isospin mixing between the  $T = 3/2, J^\pi = 3/2^-$  IAS of  $^{55}\text{Cu}$  and a very close-lying  $T = 1/2, J^\pi = 3/2^-$  state was observed in a  $\beta$ -decay experiment leading to  $^{55}\text{Ni}$  [42]. Very similar observations had been made in the 1970s for the IAS of  $^{55}\text{Fe}$  in the mirror nucleus  $^{55}\text{Co}$  [28,29,43]. The recent  $\beta$ -decay data on  $^{55}\text{Ni}$  hint at slightly stronger isospin mixing in  $^{55}\text{Co}$  [42] as compared to the earlier work mentioned above. The degree of isospin mixing between  $T = 0$  and  $T = 1$  components in the ground state of  $^{56}\text{Ni}$  has been controversially discussed. Some evidence comes from the detection of  $\beta$ -delayed protons after the  $\beta^+$  decay of  $^{57}\text{Zn}$  ( $T = 3/2$ ), where both the  $0_1^+$  and  $2_1^+$  states in  $^{56}\text{Ni}$  ( $T = 0$ ) were strongly populated [44].

Here, we investigate the single-particle structure of self-conjugate  $^{56}\text{Ni}$  and the mirrors  $^{55}\text{Ni}$  ( $^{55}\text{Co}$ ) using the  $\gamma$ -ray-tagged mirrored one-neutron (one-proton) knockout reactions. Mirror asymmetries in partial cross sections and  $\gamma$ -decay patterns will be discussed.

The experiment was performed at the Coupled Cyclotron Facility of the National Superconducting Cyclotron Laboratory (NSCL) at Michigan State University [45]. The secondary beam of  $^{56}\text{Ni}$  was selected in flight with the A1900 fragment separator [46] using a  $300 \text{ mg/cm}^2$  Al degrader after production from a  $160 \text{ MeV/u}$   $^{58}\text{Ni}$  primary beam in projectile fragmentation on a thick  $610 \text{ mg/cm}^2$   $^9\text{Be}$  target. The  $^{56}\text{Ni}$  secondary beam was unambiguously distinguished from the  $^{55}\text{Co}$  (27%) and  $^{54}\text{Fe}$  (1%) contaminants via the time-of-flight difference measured between two plastic scintillators located at the exit of the A1900 and the object position of the S800 analysis beam line. A  $188 \text{ mg/cm}^2$   $^9\text{Be}$  reaction target was surrounded by the SeGA array consisting of 16 32-fold segmented high-purity germanium detectors [47]. The detectors were arranged in two rings with central angles of  $37^\circ$  (7 detectors) and  $90^\circ$  (9 detectors) relative to the beam axis. The segmentation of the detectors enables an event-by-event Doppler reconstruction of the  $\gamma$  rays emitted by the projectile-like reaction residues in flight ( $v/c \approx 0.4$ ). The angle of the  $\gamma$ -ray emission needed for this reconstruction is determined from the segment position that registered the highest energy deposition. All projectile-like reaction residues entering the S800 focal plane were identified event by event from their energy loss and time of flight [48]. The Doppler-corrected in-beam  $\gamma$ -ray singles spectra in coincidence with event-by-event identified knockout residues are shown in Fig. 1. Only a change in magnetic rigidity of the S800 spectrograph was required to switch from one knockout setting to the other.

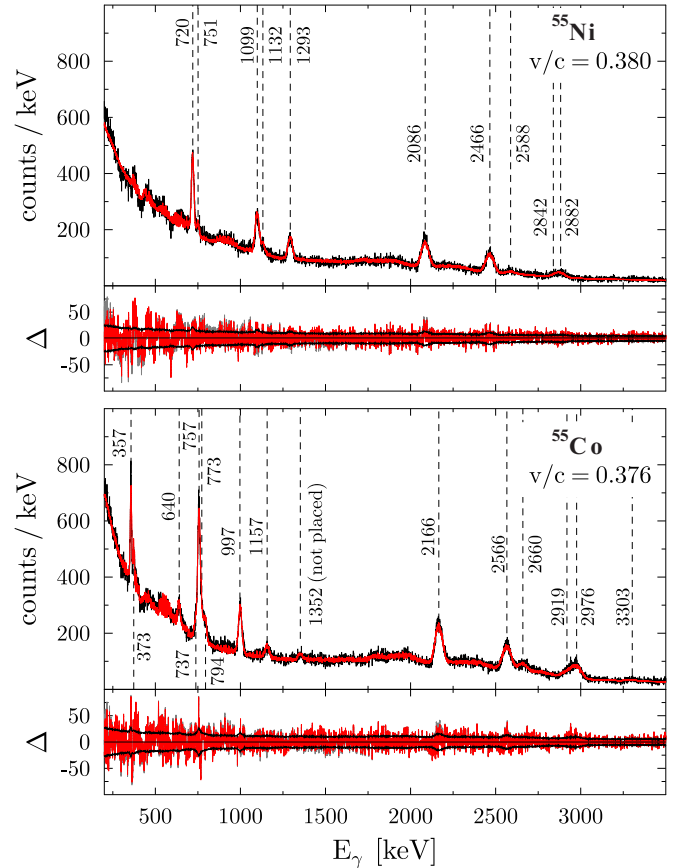


FIG. 1. In-beam  $\gamma$ -ray singles spectra for  $^{55}\text{Ni}$  (top) and  $^{55}\text{Co}$  (bottom) in black compared to  $\gamma$ -ray spectra obtained from a GEANT4 simulation (red). Observed transitions are marked with dashed vertical lines and their corresponding transition energies. Also shown are the fit residuals  $\Delta$  (red) in combination with the  $1\sigma$  confidence level (black) in the lower panels. The background structures between 400 and 800 keV, seen on top of the smooth background, are caused by  $\gamma$  rays emitted from stopped components and taken into account in the simulation.

Inclusive cross sections of  $38.0 \pm 0.2$  (stat.)  $\pm 3.0$  (sys.) mb for the one-neutron knockout from  $^{56}\text{Ni}$  to all bound states of  $^{55}\text{Ni}$  and of  $126 \pm 2$  (stat.)  $\pm 17$  (sys.) mb for the one-proton knockout to all bound final states of  $^{55}\text{Co}$  were determined. In both cases, the inclusive cross section was deduced from the yield of the detected knockout residues relative to the number of incoming  $^{56}\text{Ni}$  projectiles and the number density of the  $^9\text{Be}$  reaction target. Statistical and systematic uncertainties are quoted separately. The latter include the stability of the secondary beam composition, the choice of software gates, and corrections for acceptance losses in the tails of the residue parallel momentum distributions due to the blocking of the unreacted beam in the focal plane. The parallel momentum distribution of the knockout residues was reconstructed on an event-by-event basis using the two position-sensitive cathode readout drift counters of the S800 focal-plane detection system [48] in conjunction with trajectory reconstruction through the spectrograph.

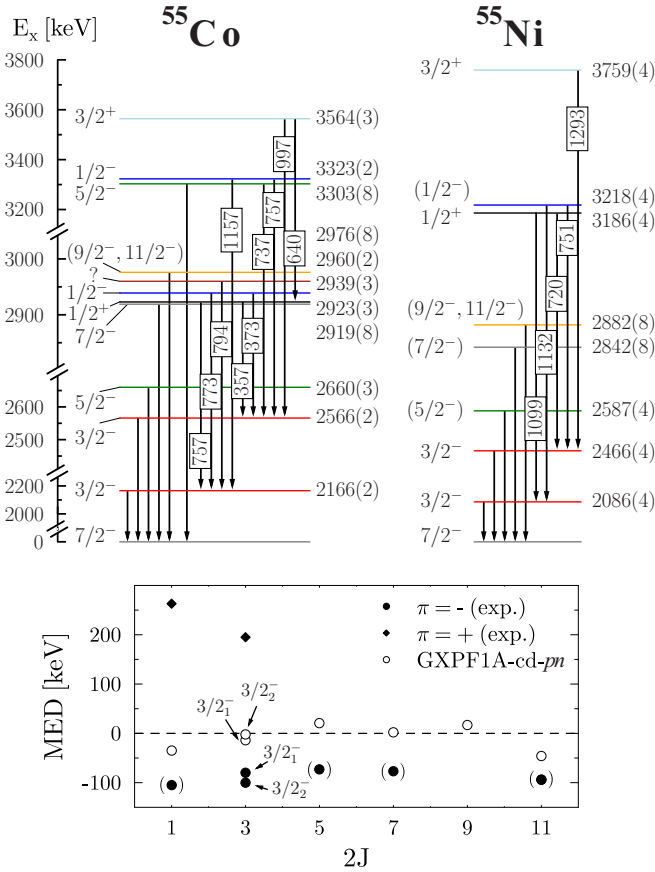


FIG. 2. Level scheme observed for  $^{55}\text{Co}$  and  $^{55}\text{Ni}$ . All transitions visible in Fig. 1 with the exception of the 1352 keV ( $^{55}\text{Co}$ ) transition are placed. The color coding is the same as in Fig. 3. The bottom panel shows the calculated MED for the two  $3/2^-$  and the  $5/2^-$ ,  $1/2^-$ ,  $7/2^-$ , and  $(9/2^-, 11/2^-)$  states (solid circles) as well as the  $1/2^+$  and  $3/2^+$  states (solid diamonds) in comparison to the shell-model results (open circles,  $pf$  states only). Even though the transition intensities seen in Fig. 1 are comparable, the MED for the excited  $J^\pi = 5/2^-$ ,  $1/2^-$ ,  $7/2^-$ , and  $(9/2^-, 11/2^-)$  states are only tentatively assigned and, thus, shown in parentheses. Except for the  $3/2^+$  state discussed in the text,  $J^\pi$  assignments were adopted from Refs. [27,36,42].

To calculate the  $\gamma$ -ray yields needed to determine the partial cross sections to individual final states, GEANT4 simulations were performed with the UCSeGA simulation package [49]. The results of those simulations, assuming a smooth double-exponential background, are shown in Fig. 1 together with the measured  $\gamma$ -ray spectra. Possible sources of the in-beam background were discussed in, e.g., [50–52]. Using  $\gamma\gamma$  coincidences, feeders were identified and the placement of previously known  $\gamma$ -ray transitions in the level scheme [27,42] confirmed. The level schemes are displayed in Fig. 2.

Partial cross sections to individual final excited states in  $^{55}\text{Ni}$  and  $^{55}\text{Co}$ , feeding-corrected where possible, are presented in Figs. 3(a) and 3(b) along with the corresponding predictions of calculations in Figs. 3(c) and 3(d), combining shell-model spectroscopic factors with eikonal reaction theory [53] following the approach outlined in [54,55]. As

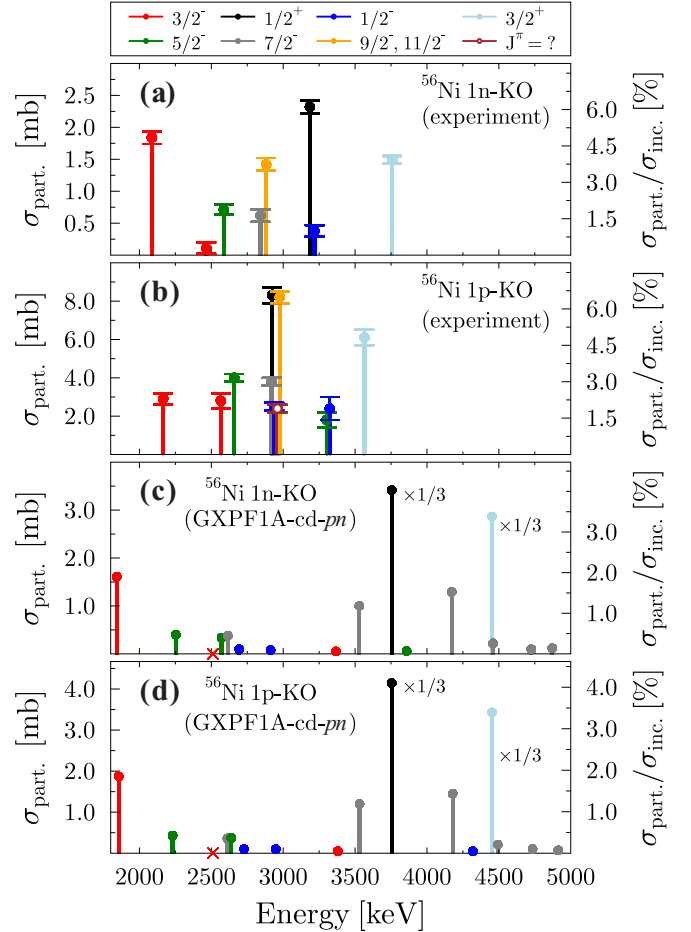


FIG. 3. Partial cross sections  $\sigma_{\text{part}}$  determined for (a)  $^{55}\text{Ni}$  and (b)  $^{55}\text{Co}$  in comparison to (c), (d) the theoretical cross sections. Only states predicted with  $\sigma_{\text{part}} \geq 0.05$  mb are presented. The spectroscopic factors and excitation energies predicted for the  $1/2^+$  and  $3/2^+$  state have been taken from Ref. [36]. The location of the  $3/2^-$  state is indicated by a red cross ( $\sigma_{\text{part}} \approx 0.01$  mb). In addition, the partial cross sections relative to the inclusive cross section  $\sigma_{\text{inc}}$  are shown, see second axis. Only statistical uncertainties are given. No reduction factor  $R_s$  has been applied for the comparison. See text for further details.

input for the cross-section calculations, the valence-nucleon radial wave functions were calculated in a Woods-Saxon-plus-spin-orbit potential, the geometry of which is constrained by Hartree-Fock calculations using the SkX Skyrme interaction [56]. Shell-model calculations in the full  $pf$  shell using the GXPFI1A-cd- $pn$  Hamiltonian were used to compute the spectroscopic factors  $C^2S(J^\pi)$  between the  $^{56}\text{Ni}$  ground state and final states with  $J^\pi$  in  $^{55}\text{Co}$  and  $^{55}\text{Ni}$ , which enter the knockout cross sections. GXPFI1A is the isospin conserving part as obtained in [21,57,58]. The charge-dependent (cd) Hamiltonian from [59] was added. The isotensor part of this Hamiltonian does not change the wave functions for states with  $T = 1/2$ . The total wave functions were calculated in a proton-neutron basis ( $pn$ ). For these shell-model calculations, the computer code NUSHELLX was utilized [60]. For further details on the calculation of the theoretical cross sections, see

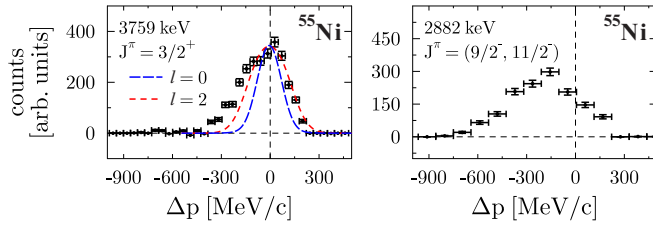


FIG. 4. Parallel momentum distributions measured for the  $J^\pi = 3/2^+$  and  $(9/2^-, 11/2^-)$  states in  $^{55}\text{Ni}$ . For the  $J^\pi = 3/2^+$  state, the predictions of the eikonal theory calculated at a mid-target energy of 85.9 MeV/u and folded with the momentum distribution of the unreacted beam passing through the target are shown with dashed lines. The parallel momentum distribution of the 2882 keV state was obtained by gating on the high-energy part of the doublet seen in Fig. 1. For both distributions, background contributions were subtracted. Very similar distributions were observed for  $^{55}\text{Co}$ . See text for further discussion.

the Supplemental Material [61]. In addition to the absolute values, partial cross sections  $\sigma_{\text{part}}$  relative to the inclusive cross section  $\sigma_{\text{inc}}$  are shown in Fig. 3. The ground-state partial cross sections obtained from subtraction are 29.1(7) mb [77(2)%] in  $^{55}\text{Ni}$  and 80(5) mb [63(4)%] in  $^{55}\text{Co}$ . Those values are upper limits only due to the possibility of missed, weak feeding transitions.

For the states observed in this work, the MED are shown for completeness in the lower panel of Fig. 2 in comparison to the shell-model predictions with the GXPF1A-cd- $pn$  Hamiltonian ( $pf$  states only). The theoretical MED differ by 50–80 keV. The negative values of the MED relative to the  $A = 55$  ground states might be interpreted in terms of an increase in the mean nuclear radii of the excited states relative to that of the ground state due to the increased occupancy of the  $2p_{3/2}$  orbital and the connected contribution to the MED through changes in the bulk Coulomb energy from the difference in  $Z$  between the mirrors [3,62]. This corresponds to the influence of the monopole radial term on the MED [3]. An MED of  $-100$  keV corresponds to a 1.0% increase in the radius. This effect of an increased  $2p_{3/2}$  occupancy on the charge radius is similar to the isotope shift of 1.2% observed between  $^{56}\text{Fe}$  and  $^{54}\text{Fe}$  [63]. The MED for the  $1/2^+$  and  $3/2^+$  states relative to the  $7/2^-$  ground state also show that the addition of the relativistic spin-orbit correction of order +100 to +200 keV (see Table IV in [64]) as well as the correction for the Coulomb energy stored in a single-proton orbital are required [62], which corresponds to the influence of the monopole single-particle term on the MED [3]. In both nuclei, the  $1/2^+$  and  $3/2^+$  states are comparably strongly populated [see Figs. 3(a) and 3(b)]. These states are expected to have significant contributions to their wave function from the  $sd$  orbitals below the  $N = Z = 28$  shell closure and have been previously discussed in [36], where the  $1/2^+$  state in  $^{55}\text{Ni}$  was also strongly populated. The  $3/2_1^+$  state had not been unambiguously identified [27,36]. The measured parallel momentum distributions, see Fig. 4 for  $^{55}\text{Ni}$ , support a  $3/2^+$  assignment based on the clear observation of a nucleon knockout from an  $l = 2$  orbital.

It is interesting to note that the possible  $(9/2^-, 11/2^-)$  doublet of the  $2_1^+$  ( $^{56}\text{Ni}$ )  $\otimes 1f_{7/2}^{-1}$  multiplet is weakly populated in this work, 1.42(10) mb [3.7(3)%] in  $^{55}\text{Ni}$  and 8.2(3) mb [6.5(2)%] in  $^{55}\text{Co}$ . The population of these states cannot proceed by a one-step knockout process from the  $^{56}\text{Ni}$  ground state. The population of such complex configurations has been reported before, possibly due to the knockout from the  $2_1^+$  state of the projectile (see the discussion in [50,65]). It has been speculated in previous studies that such indirect reaction mechanisms result in downshifts observed for some parallel-momentum distributions [50,65]. As is shown in Fig. 4, the distributions for those states are indeed shifted to lower momenta while the simpler configurations such as the main fragment of the  $1d_{3/2}$  state line up as expected from the eikonal theory. The structure assignment is supported by the observation of  $B(E2; (9/2^-, 11/2^-) \rightarrow 7/2_1^-)$  values similar to the  $B(E2; 2_1^+ \rightarrow 0_1^+)$  of  $^{56}\text{Ni}$  [27,41]. The present shell-model calculations predict large spectroscopic factors between the  $2_1^+$  state of  $^{56}\text{Ni}$  and the  $(9/2^-, 11/2^-)$  states in the  $A = 55$  nuclei of  $C^2S = 1.62$  and 1.12, respectively. Theoretically, these core-coupled states are located at energies of about 2.8 MeV.

We note that a discussion of the reduction factor  $R_s = \sigma_{\text{expt}}/\sigma_{\text{th}}$ , reported for a large body of consistently analyzed knockout reactions [54,55], is not very instructive here as knockout from the  $sd$  shell is observed, which is outside of the model space employed by the present shell-model calculations. Nevertheless, we can make a consistency argument. The theoretically expected inclusive cross sections, including the  $1/2^+$  and  $3/2^+$  states with spectroscopic factors from Ref. [36], are 85 mb in  $^{55}\text{Ni}$  and 101 mb in  $^{55}\text{Co}$ . For  $^{55}\text{Ni}$  this gives a reduction factor of  $R_s = 0.45(4)$  ( $\Delta S = 10.5$  MeV), consistent with expectations from [54,55]. For the slightly more deeply bound  $^{55}\text{Co}$  ( $S_p > 5$  MeV), we expect that more bound  $sd$ -shell strength has to be included. Based on  $^{57}\text{Co}$  [66], the  $2s_{1/2}$  strength may be fully exhausted and 75% of the  $1d_{3/2}$  strength may be found below 5.2 MeV. Assuming in addition a spectroscopic factor of 1 for the bound  $1d_{5/2}$  strength, and subtracting the cross section of the indirect contribution identified above, leads to a reduction factor of 0.93(13) consistent with [54,55].

Besides the slightly stronger relative population of the  $5/2_1^-$ ,  $7/2_2^-$ ,  $(9/2^-, 11/2^-)$ , and  $1/2_2^-$  states in  $^{55}\text{Co}$ , the fragmentation of the spectroscopic strengths between the two lowest-lying  $3/2^-$  states is very different [see Figs. 3(a) and 3(b)]. One has to consider that this difference may be caused by unobserved feeding ( $^{55}\text{Co}$  is slightly more bound than  $^{55}\text{Ni}$  and will consequently have more bound excited states). For instance, the unplaced 1352 keV transition, if feeding the 2566 keV level, would decrease its direct partial cross section by  $\approx 33\%$ . The  $\gamma$ -ray yields needed for resolved transitions over an energy range from 0.5 to 3 MeV to obtain comparable cross sections for the  $3/2^-$  states due to unaccounted feeding were estimated. If collected in a single or even two transitions, all of those feeders should have been identified in the  $\gamma$ -ray singles spectra. If this asymmetry was indeed caused by different feeding, the needed strength would have to be fragmented over multiple transitions which all have to



be below the detection limit of the present measurement. It should be mentioned that the number of levels observed to feed the  $3/2^-$  state in  $^{55}\text{Co}$  is larger than in  $^{55}\text{Ni}$  (compare Fig. 2). Still, after subtraction, its partial cross section is larger.

The observed asymmetry in the partial cross sections is theoretically not expected for the  $3/2^-$  states [compare Figs. 3(c) and 3(d)]. Therefore, spectroscopic factors  $C^2S$  for the one proton transfer from  $^{54}\text{Fe}$  (ground state) to  $^{55}\text{Co}$  ( $J^\pi = 3/2^-$ ) were also calculated and compared to the data from Table 1 of [29]. To obtain agreement between the shell-model spectroscopic factors and the experimentally determined ratio of  $C^2S(3/2^-_1)/C^2S(3/2^-_2) = 1.54(22)$  in  $^{55}\text{Co}$ , derived as the average from several  $^{54}\text{Fe}$  to  $^{55}\text{Co}$  transfer reactions [29], mixing amplitudes of  $\alpha = 0.995^{+0.003}_{-0.004}$  ( $\alpha^2 = 0.990^{+0.005}_{-0.010}$ ) and  $\beta = -0.10^{+0.04}_{-0.03}$  ( $\beta^2 = 0.010^{+0.010}_{-0.005}$ ) result in a model with two unperturbed  $3/2^-$  ( $j = I, II$ ) states. The wave functions of the mixed states are then given by

$$\begin{aligned} |3/2^-_1\rangle &= \alpha|3/2^-_I\rangle + \beta|3/2^-_{II}\rangle, \\ |3/2^-_2\rangle &= -\beta|3/2^-_I\rangle + \alpha|3/2^-_{II}\rangle, \end{aligned}$$

Without introducing this 0.5% to 2% mixing, the ratio between the corresponding shell-model spectroscopic factors would have been 2.35 [ $C^2S(3/2^-_1) = 1.22$ ,  $C^2S(3/2^-_2) = 0.52$ ]. Applying the same mixing to the one-proton knockout from the  $^{56}\text{Ni}$  ground state to  $^{55}\text{Co}$  leads to spectroscopic factors of  $0.181^{+0.002}_{-0.003}$  for  $3/2^-_1$  and  $0.006^{+0.003}_{-0.002}$  for  $3/2^-_2$  (0.186 and 0.001 without mixing), respectively, not explaining the asymmetry in the partial cross sections reported here. The emerging contradictory picture prevents conclusions on the role of isospin mixing based on the asymmetry in the partial cross sections,  $\sigma(3/2^-_i)$ , and suggests that unobserved feeding in the present data may indeed be a contributor.

However, independent of the cross-section discussion, the  $\gamma$ -decay pattern of the  $1/2^+$  state, which is the main feeder of the  $3/2^-$  levels, is also significantly different in the two mirror nuclei. The phase-space corrected  $R(E1)_{3/2^-_2/3/2^-_1}$  ratios are 2.69(14) and 3.9(3) in  $^{55}\text{Co}$  and  $^{55}\text{Ni}$ , respectively. To put this into perspective, these numbers mean that  $\approx 18\%$  of the feeding-uncorrected  $\gamma$ -ray yield of the  $3/2^-_2$  state in  $^{55}\text{Co}$  is due to the decay of the  $1/2^+$  state while this contribution is  $\approx 55\%$  in  $^{55}\text{Ni}$  ( $\approx 50\%$  and  $\approx 48\%$  for the  $3/2^-_1$ ). The adopted lifetime of  $\tau = 71^{+260}_{-4}$  fs [27] and the newly determined branching ratio in  $^{55}\text{Co}$  allowed us to calculate the reduced  $B(E1; 1/2^+ \rightarrow 3/2^-_i)$  transition strengths to be  $17.2^{+1.2}_{-13.5}$  mW.u. to the  $3/2^-_1$  and  $46^{+4}_{-36}$  mW.u. to the  $3/2^-_2$ , respectively. For low-lying  $E1$  transitions, such rates are, despite the large uncertainty of the lifetime, significantly enhanced. As mentioned in the introduction, a clear change of the  $E1$ -decay behavior of an excited state between mirror nuclei, as observed here, has been attributed to isospin-mixing effects in the  $A = 35$  [4] and 67 [7] mirror pairs.

With the mixing amplitudes determined from the  $^{54}\text{Fe}$ - $^{55}\text{Co}$  transfer data, two solutions for the unperturbed matrix elements  $\langle 3/2^-_{I,II} | T(E1) | 1/2^+ \rangle$  can be obtained. The uncertainty of the absolute  $B(E1)$  strengths due to the lifetime uncertainty is neglected in the following discussion. It will affect both values in the same way and, thus, not change the

ratio between them. In the first case, both matrix elements are positive and large, leading to  $B(E1; 1/2^+ \rightarrow 3/2^-_{I,II})$  values of 23(3) mW.u. for the first and 40(3) mW.u. for the second unperturbed  $3/2^-$  state. In the second case, where one of the  $E1$  matrix elements is negative,  $B(E1)$  values of 12(3) mW.u. and 51(3) mW.u. are obtained. In both cases the first  $E1$  matrix element is also comparably large. We note that an  $E1$  transition between pure  $(2s_{1/2})^{-1}(1f_{7/2})^8$  hole and  $(1f_{7/2})^6(2p_{3/2})^1$  particle configurations for the  $1/2^+$  and  $3/2^-$ , respectively, would be forbidden. Consequently, more complex configurations have to be present to explain the enhanced  $E1$  rates. In fact, the relative partial cross sections of 6.1(3)% in  $^{55}\text{Ni}$  and 6.6(3)% in  $^{55}\text{Co}$  are almost identical for the  $1/2^+$  state (compare Fig. 3), which suggests a similar structure of the  $1/2^+$  state in the mirror pair and supports the hypothesis that the observed change in the  $E1$  decay pattern probes the degree of mixing between the two  $3/2^-$  states. The amount of isospin mixing needed to explain the  $E1$  asymmetry for a low-lying  $7/2^-$  level in the  $A = 35$  and a  $9/2^+$  state in the  $A = 67$  mirror nuclei was estimated to be on the order of 1–5% [4,7–9]. In contrast to Refs. [4,7–9], no mixing for the initial and final states but only between the two final states was assumed in the mixing scenario discussed here. Interestingly, the unperturbed  $R(E1)_{3/2^-_2/3/2^-_1}$  ratio is  $4.3^{+1.7}_{-1.1}$  in the second case, i.e., closer to the experimentally observed ratio for  $^{55}\text{Ni}$ . The smaller experimentally observed  $R(E1)$  ratio in  $^{55}\text{Co}$  might, thus, point at stronger mixing between the unperturbed  $3/2^-$  states than in its mirror  $^{55}\text{Ni}$ .

In conclusion, we have performed the first mirrored one-nucleon knockout reactions on the self-conjugate nucleus  $^{56}\text{Ni}$  leading to the mirror pair ( $^{55}\text{Ni}$ ,  $^{55}\text{Co}$ ). From in-beam  $\gamma$ -ray spectroscopy, partial cross sections were determined and the  $\gamma$ -decay properties were studied for a number of excited states in  $^{55}\text{Ni}$  and  $^{55}\text{Co}$ . Several states carrying single-particle strength were populated in the  $A = 55$  mirror pair. The fragments of the  $2s_{1/2}$  and  $1d_{3/2}$  hole states carry significant cross sections in both nuclei, emphasizing the necessity to include  $sd$  orbitals for the description of nuclei in this region. Small cross sections to a potential doublet of core-coupled states [ $2^+_{1/2} (^{56}\text{Ni}) \otimes 1f_{7/2}^{-1}$ ], ( $9/2^-$ ,  $11/2^-$ ), were also observed, together with a telltale downshift in their parallel momentum distributions, indicative of an indirect reaction pathway. A pronounced cross-section asymmetry for the two lowest-lying  $3/2^-$  states as well as a clear change in the  $E1$  decay pattern of the  $1/2^+$  level feeding the  $3/2^-$  states were discussed. The high degree of mixing that would be needed to explain the cross-section asymmetry in a two-level approach cannot be reconciled with a comparison of data on the transfer from  $^{54}\text{Fe}$  to  $^{55}\text{Co}$  to the corresponding shell-model calculations, thus preventing conclusions on the role of isospin mixing. The change in the  $E1$  decay pattern, however, hints at stronger mixing between the  $3/2^-$  states in  $^{55}\text{Co}$  than in its mirror  $^{55}\text{Ni}$  and reveals an unexpected mirror asymmetry close to the nominally doubly magic  $N = Z$  nucleus  $^{56}\text{Ni}$ .

M.S. thanks S. Giuliani, G. Potel and J. Rotureau for helpful discussions. This work was supported by the National Science Foundation under Grants No. PHY-1565546

(NSCL) and No. PHY-1811855, the DOE National Nuclear Security Administration through the Nuclear Science and Security Consortium under Award No. DE-NA0003180 as

well as by the UK Science and Technology Facilities Council (STFC) through Research Grants No. ST/F005314/1, No. ST/P003885/1, and No. GR/T18486/01.

- [1] D. D. Warner, M. A. Bentley, and P. van Isacker, *Nat. Phys.* **2**, 311 (2006).
- [2] M. Bentley and S. Lenzi, *Prog. Part. Nucl. Phys.* **59**, 497 (2007).
- [3] M. A. Bentley, S. M. Lenzi, S. A. Simpson, and C. A. Diget, *Phys. Rev. C* **92**, 024310 (2015).
- [4] J. Ekman, D. Rudolph, C. Fahlander, A. P. Zuker, M. A. Bentley, S. M. Lenzi, C. Andreoiu, M. Axiotis, G. de Angelis, E. Farnea, A. Gadea, T. Kröll, N. Märginean, T. Martinez, M. N. Mineva, C. Rossi-Alvarez, and C. A. Ur, *Phys. Rev. Lett.* **92**, 132502 (2004).
- [5] D. G. Jenkins, C. J. Lister, M. P. Carpenter, P. Chowdhury, N. J. Hammond, R. V. F. Janssens, T. L. Khoo, T. Lauritsen, D. Seweryniak, T. Davinson, P. J. Woods, A. Jokinen, and H. Penttilä, *Phys. Rev. C* **72**, 031303(R) (2005).
- [6] M. A. Bentley, C. Chandler, P. Bednarczyk, F. Brandolini, A. M. Bruce, D. Curien, O. Dorvaux, J. Ekman, E. Farnea, W. Gelletly, D. T. Joss, S. M. Lenzi, D. R. Napoli, J. Nyberg, C. D. O’Leary, S. J. Williams, and D. D. Warner, *Phys. Rev. C* **73**, 024304 (2006).
- [7] R. Orlandi, G. de Angelis, P. G. Bizzeti, S. Lunardi, A. Gadea, A. M. Bizzeti-Sona, A. Bracco, F. Brandolini, M. P. Carpenter, C. J. Chiara, F. Della Vedova, E. Farnea, J. P. Greene, S. M. Lenzi, S. Leoni, C. J. Lister, N. Märginean, D. Mengoni, D. R. Napoli, B. S. N. Singh, O. L. Pechenaya, F. Recchia, W. Reviol, E. Sahin, D. G. Sarantites, D. Seweryniak, D. Tonev, C. A. Ur, J. J. Valiente-Dobón, R. Wadsworth, K. T. Wiedemann, and S. Zhu, *Phys. Rev. Lett.* **103**, 052501 (2009).
- [8] N. S. Pattabiraman, D. G. Jenkins, M. A. Bentley, R. Wadsworth, C. J. Lister, M. P. Carpenter, R. V. F. Janssens, T. L. Khoo, T. Lauritsen, D. Seweryniak, S. Zhu, G. Lotay, P. J. Woods, Krishichayan, and P. V. Isacker, *Phys. Rev. C* **78**, 024301 (2008).
- [9] P. G. Bizzeti, G. de Angelis, S. M. Lenzi, and R. Orlandi, *Phys. Rev. C* **86**, 044311 (2012).
- [10] P. J. Davies, M. A. Bentley, T. W. Henry, E. C. Simpson, A. Gade, S. M. Lenzi, T. Baugher, D. Bazin, J. S. Berryman, A. M. Bruce, C. A. Diget, H. Iwasaki, A. Lemasson, S. McDaniel, D. R. Napoli, A. Ratkiewicz, L. Scruton, A. Shore, R. Stroberg, J. A. Tostevin, D. Weisshaar, K. Wimmer, and R. Winkler, *Phys. Rev. Lett.* **111**, 072501 (2013).
- [11] S. A. Milne, M. A. Bentley, E. C. Simpson, P. Dodsworth, T. Baugher, D. Bazin, J. S. Berryman, A. M. Bruce, P. J. Davies, C. A. Diget, A. Gade, T. W. Henry, H. Iwasaki, A. Lemasson, S. M. Lenzi, S. McDaniel, D. R. Napoli, A. J. Nichols, A. Ratkiewicz, L. Scruton, S. R. Stroberg, J. A. Tostevin, D. Weisshaar, K. Wimmer, and R. Winkler, *Phys. Rev. C* **93**, 024318 (2016).
- [12] K. Wimmer, W. Korten, T. Arici, P. Doornenbal, P. Aguilera, A. Algora, T. Ando, H. Baba, B. Blank, A. Boso, S. Chen, A. Corsi, P. Davies, G. de Angelis, G. de France, D. Doherty, J. Gerl, R. Gernhäuser, D. Jenkins, S. Koyama, T. Motobayashi, S. Nagamine, M. Niikura, A. Obertelli, D. Lubos, B. Rubio, E. Sahin, T. Saito, H. Sakurai, L. Sinclair, D. Steppenbeck, R. Taniuchi, R. Wadsworth, and M. Zielinska, *Phys. Lett. B* **785**, 441 (2018).
- [13] J. R. Brown, M. A. Bentley, P. Adrich, D. Bazin, J. M. Cook, C. A. Diget, A. Gade, T. Glasmacher, S. M. Lenzi, S. McDaniel, B. Pritychenko, A. Ratkiewicz, K. Siwek, M. J. Taylor, and D. Weisshaar, *Phys. Rev. C* **80**, 011306(R) (2009).
- [14] G. Hagen, M. Hjorth-Jensen, G. R. Jansen, and T. Papenbrock, *Phys. Scr.* **91**, 063006 (2016).
- [15] H. Hergert, *Phys. Scr.* **92**, 023002 (2017).
- [16] M. Horoi, B. A. Brown, T. Otsuka, M. Honma, and T. Mizusaki, *Phys. Rev. C* **73**, 061305(R) (2006).
- [17] M. Horoi, J. R. Gour, M. Włoch, M. D. Lodirosso, B. A. Brown, and P. Piecuch, *Phys. Rev. Lett.* **98**, 112501 (2007).
- [18] J. R. Gour, M. Horoi, P. Piecuch, and B. A. Brown, *Phys. Rev. Lett.* **101**, 052501 (2008).
- [19] C. Barbieri, *Phys. Rev. Lett.* **103**, 202502 (2009).
- [20] C. Barbieri and M. Hjorth-Jensen, *Phys. Rev. C* **79**, 064313 (2009).
- [21] M. Honma, T. Otsuka, B. A. Brown, and T. Mizusaki, *Phys. Rev. C* **69**, 034335 (2004).
- [22] K. L. Yurkewicz, D. Bazin, B. A. Brown, C. M. Campbell, J. A. Church, D. C. Dinca, A. Gade, T. Glasmacher, M. Honma, T. Mizusaki, W. F. Mueller, H. Olliver, T. Otsuka, L. A. Riley, and J. R. Terry, *Phys. Rev. C* **70**, 054319 (2004).
- [23] P. Callaghan, M. Kaplan, and N. Stone, *Nucl. Phys. A* **201**, 561 (1973).
- [24] T. Ohtsubo, D. J. Cho, Y. Yanagihashi, S. Ohya, and S. Muto, *Phys. Rev. C* **54**, 554 (1996).
- [25] J. S. Berryman, K. Minamisono, W. F. Rogers, B. A. Brown, H. L. Crawford, G. F. Grinyer, P. F. Mantica, J. B. Stoker, and I. S. Towner, *Phys. Rev. C* **79**, 064305 (2009).
- [26] T. E. Cocolios, A. N. Andreyev, B. Bastin, N. Bree, J. Büscher, J. Elseviers, J. Gentens, M. Huyse, Y. Kudryavtsev, D. Pauwels, T. Sonoda, P. Van den Bergh, and P. Van Duppen, *Phys. Rev. Lett.* **103**, 102501 (2009).
- [27] ENSDF, NNDC Online Data Service, ENSDF database, <http://www.nndc.bnl.gov/ensdf/> (2019).
- [28] R. Shoup, J. Fox, R. Brown, G. Vourvopoulos, and S. Maripuu, *Nucl. Phys. A* **183**, 21 (1972).
- [29] S. Fortier, J. Maison, S. Galés, H. Laurent, and J. Schapira, *Nucl. Phys. A* **288**, 82 (1977).
- [30] B. Erlandsson and J. Lyttkens, *Z. Phys. A* **280**, 79 (1977).
- [31] X. G. Zhou, H. Dejbakhsh, C. A. Gagliardi, J. Jiang, L. Trache, and R. E. Tribble, *Phys. Rev. C* **53**, 982 (1996).
- [32] K. L. Yurkewicz, D. Bazin, B. A. Brown, J. Enders, A. Gade, T. Glasmacher, P. G. Hansen, V. Maddalena, A. Navin, B. M. Sherrill, and J. A. Tostevin, *Phys. Rev. C* **74**, 024304 (2006).
- [33] C. L. Jiang, K. E. Rehm, D. Ackermann, I. Ahmad, J. P. Greene, B. Harss, D. Henderson, W. F. Henning, R. V. F. Janssens, J. Nolen, R. C. Pardo, P. Reiter, J. P. Schiffer, D. Seweryniak, A. Sonzogni, J. Usitalo, I. Wiedenhöver, A. H. Wuosmaa, F. Brumwell, G. McMichael, M. Paul, and R. E. Segel, *Phys. Rev. C* **80**, 044613 (2009).
- [34] J. Lee, M. B. Tsang, W. G. Lynch, M. Horoi, and S. C. Su, *Phys. Rev. C* **79**, 054611 (2009).
- [35] J. P. Schiffer, C. R. Hoffman, B. P. Kay, J. A. Clark, C. M. Deibel, S. J. Freeman, M. Honma, A. M. Howard, A. J.

- Mitchell, T. Otsuka, P. D. Parker, D. K. Sharp, and J. S. Thomas, *Phys. Rev. C* **87**, 034306 (2013).
- [36] A. Sanetullaev, M. Tsang, W. Lynch, J. Lee, D. Bazin, K. Chan, D. Coupland, V. Henzl, D. Henzlova, M. Kilburn, A. Rogers, Z. Sun, M. Youngs, R. Charity, L. Sobotka, M. Famiano, S. Hudan, D. Shapira, W. Peters, C. Barbieri, M. Hjorth-Jensen, M. Horoi, T. Otsuka, T. Suzuki, and Y. Utsuno, *Phys. Lett. B* **736**, 137 (2014).
- [37] L. Trache, A. Kolomiets, S. Shlomo, K. Heyde, H. Dejbakhsh, C. A. Gagliardi, R. E. Tribble, X. G. Zhou, V. E. Iacob, and A. M. Oros, *Phys. Rev. C* **54**, 2361 (1996).
- [38] E. V. Litvinova and A. V. Afanasjev, *Phys. Rev. C* **84**, 014305 (2011).
- [39] K. S. Burton and L. C. McIntyre, *Phys. Rev. C* **3**, 621 (1971).
- [40] E. Brookes and B. Robertson, *Nucl. Phys. A* **462**, 527 (1987).
- [41] K. L. Yurkewicz, D. Bazin, B. A. Brown, C. M. Campbell, J. A. Church, D.-C. Dinca, A. Gade, T. Glasmacher, M. Honma, T. Mizusaki, W. F. Mueller, H. Olliver, T. Otsuka, L. A. Riley, and J. R. Terry, *Phys. Rev. C* **70**, 064321 (2004).
- [42] V. Tripathi, S. L. Tabor, A. Volya, S. N. Liddick, P. C. Bender, N. Larson, C. Prokop, S. Suchyta, P.-L. Tai, and J. M. VonMoss, *Phys. Rev. Lett.* **111**, 262501 (2013).
- [43] D. Martin, W. McLatchie, B. Robertson, and J. Szücs, *Nucl. Phys. A* **258**, 131 (1976).
- [44] A. Jokinen, A. Nieminen, J. Äystö, R. Borcea, E. Caurier, P. Dendooven, M. Gierlik, M. Górska, H. Grawe, M. Hellström, M. Karny, Z. Janas, R. Kirchner, M. L. Commara, G. Martínez-Pinedo, P. Mayet, H. Penttilä, A. Plochocki, M. Rejmund, E. Roeckl, M. Sawicka, C. Schlegel, K. Schmidt, and R. Schwengner, *EPJdirect* **4**, 1 (2002).
- [45] A. Gade and B. Sherrill, *Phys. Scr.* **91**, 053003 (2016).
- [46] D. Morrissey, B. Sherrill, M. Steiner, A. Stolz, and I. Wiedenhoever, *Nucl. Instrum. Methods B* **204**, 90 (2003).
- [47] W. Mueller, J. Church, T. Glasmacher, D. Gutknecht, G. Hackman, P. Hansen, Z. Hu, K. Miller, and P. Quirin, *Nucl. Instr. and Meth. A* **466**, 492 (2001).
- [48] D. Bazin, J. Caggiano, B. Sherrill, J. Yurkon, and A. Zeller, *Nucl. Instrum. Methods B* **204**, 629 (2003).
- [49] UCSeGA GEANT4, L. A. Riley, Ursinus College (unpublished).
- [50] S. R. Stroberg, A. Gade, J. A. Tostevin, V. M. Bader, T. Baugher, D. Bazin, J. S. Berryman, B. A. Brown, C. M. Campbell, K. W. Kemper, C. Langer, E. Lunderberg, A. Lemasson, S. Noji, F. Recchia, C. Walz, D. Weisshaar, and S. J. Williams, *Phys. Rev. C* **90**, 034301 (2014).
- [51] Z. Podolyák, P. Regan, P. Walker, M. Caamaño, K. Gladnishki, J. Gerl, M. Hellström, P. Mayet, M. Pfützner, and M. Mineva, *Nucl. Phys. A* **722**, C273 (2003).
- [52] D. Weisshaar, M. Wallace, P. Adrich, D. Bazin, C. Campbell, J. Cook, S. Etenauer, A. Gade, T. Glasmacher, S. McDaniel, A. Obertelli, A. Ratkiewicz, A. Rogers, K. Siwek, and S. Tornga, *Nucl. Instrum. Methods A* **594**, 56 (2008).
- [53] J. A. Tostevin, *Nucl. Phys. A* **682**, 320 (2001).
- [54] A. Gade, P. Adrich, D. Bazin, M. D. Bowen, B. A. Brown, C. M. Campbell, J. M. Cook, T. Glasmacher, P. G. Hansen, K. Hosier, S. McDaniel, D. McGlinchery, A. Obertelli, K. Siwek, L. A. Riley, J. A. Tostevin, and D. Weisshaar, *Phys. Rev. C* **77**, 044306 (2008).
- [55] J. A. Tostevin and A. Gade, *Phys. Rev. C* **90**, 057602 (2014).
- [56] B. A. Brown, *Phys. Rev. C* **58**, 220 (1998).
- [57] M. Honma, T. Otsuka, B. A. Brown, and T. Mizusaki, *Phys. Rev. C* **65**, 061301(R) (2002).
- [58] M. Honma, T. Otsuka, B. A. Brown, and T. Mizusaki, *Eur. Phys. J. A* **25**, 499 (2005).
- [59] W. Ormand and B. A. Brown, *Nucl. Phys. A* **491**, 1 (1989).
- [60] B. A. Brown, *Nuclear Data Sheets* **120**, 115 (2014).
- [61] See Supplemental Material at <http://link.aps.org/supplemental/10.1103/PhysRevC.99.051304> for full details of the reaction model parameters, shell-model spectroscopy, and calculated cross sections.
- [62] A. P. Zuker, S. M. Lenzi, G. Martínez-Pinedo, and A. Poves, *Phys. Rev. Lett.* **89**, 142502 (2002).
- [63] K. Minamisono, D. M. Rossi, R. Beerwerth, S. Fritzsche, D. Garand, A. Klose, Y. Liu, B. Maaß, P. F. Mantica, A. J. Miller, P. Müller, W. Nazarewicz, W. Nörtershäuser, E. Olsen, M. R. Pearson, P.-G. Reinhard, E. E. Saperstein, C. Sumithrarachchi, and S. V. Tolokonnikov, *Phys. Rev. Lett.* **117**, 252501 (2016).
- [64] J. A. Nolan and J. P. Schiffer, *Ann. Rev. Nucl. Sci.* **19**, 471 (1969).
- [65] A. Mutschler, O. Sorlin, A. Lemasson, D. Bazin, C. Borcea, R. Borcea, A. Gade, H. Iwasaki, E. Khan, A. Lepailleur, F. Recchia, T. Roger, F. Rotaru, M. Stanoiu, S. R. Stroberg, J. A. Tostevin, M. Vandebrouck, D. Weisshaar, and K. Wimmer, *Phys. Rev. C* **93**, 034333 (2016).
- [66] K. Reiner, P. Grabmayr, G. Wagner, S. Banks, B. Lay, V. Officer, G. Shute, B. Spicer, C. Glover, W. Jones, D. Miller, H. Nann, and E. Stephenson, *Nucl. Phys. A* **472**, 1 (1987).